Design and fabrication of an imprinted wavelength-independent coupler

Kyung Su Jang
Eung Soo Kim
Chang Seok Kim
Myung Yung Jeong

Design and fabrication of an imprinted wavelength-independent coupler

Kyung Su Jang
Pusan National University
Department of Cogno-Mechatronics Engineering
Geumjeong-gu, Busan 609-735, Republic of Korea

Eung Soo Kim
Pusan University of Foreign Studies
Division of Digital-Media Engineering
Nam-gu, Busan 608-738, Republic of Korea

Chang Seok Kim
Myung Yung Jeong
Pusan National University
Department of Cogno-Mechatronics Engineering
Geumjeong-gu, Busan 609-735, Republic of Korea
E-mail: myjeong@pusan.ac.kr

Abstract. An imprinted polymeric wavelength-independent coupler (WINC), which is one of the core components used in optical fiber communications and fiber-to-the-home systems, was designed with a beam propagation method. Its designed structure has the form of the Mach–Zehnder interferometer. The polymer core size of the WINC was optimized at 8×8 μm using an imprinting technique, the hot embossing process. Optical properties of the polymeric WINC were evaluated by measuring its insertion loss and transmission spectrum. The insertion loss values for channels 1 and 2 were 3.5 and 4.2 dB, respectively, and the transmission spectrum was flat over a range of 1260 to 1640 nm. © *2012 Society of Photo-Optical Instrumentation Engineers (SPIE).* [DOI: 10.1117/1.OE.51.8.085003]

Subject terms: optical communication; nanoimprint; optical planar waveguide; wavelength-independent coupler.

Paper 120491 received Apr. 4, 2012; revised manuscript received Jul. 3, 2012; accepted for publication Jul. 3, 2012; published online Aug. 2, 2012.

1 Introduction

Multimedia data, such as that used for voice, text, images, and video, has become essential in our information-oriented society. Recently, the increased demand for these data has called for broadband convergence networks. To construct a high-speed information network, optical communication technology advances into the Tbps domain after the 2010s. This increased demand for high-speed information and communication networks require massive transmission capabilities and super-high-speed switching technologies for optical communications. Fiber-to-the-home (FTTH) systems are gaining strength all over the world and used for an access network for massive multimedia service.[1] To use FTTH more efficiently, the wavelength division multiplexing (WDM) method is required, which transmits different wavelengths at constant intervals. Therefore, the FTTH system needs not only optical fibers for data transmission but also photonic components for data distribution, switching, and routing between optical network terminals (ONT).

The photonic components can be generally divided into optical fiber components and planar waveguide components. The optical fiber components have to fuse optical fibers, so relatively large ones are too hard to integrate. So it has limited functions and other demerits. On the contrary, planar waveguide components not requiring the fusion process can carry out multiple functions, such as switching, routing, mux/demux, splitting, and filtering. Moreover, they can perform more than one function because they are easy to integrate with each other.[2]

Currently, planar waveguide devices are mainly fabricated using semiconductor process technology, i.e., photolithography and etching. However, the cost of waveguide components produced by these methods is relatively high and thus not suitable for low-cost application to FTTH systems.[3] Therefore imprinting technology has become more popular

and is considered a better patterning technology to fabricate polymeric waveguide devices because it is much simpler and easier to replicate than the semiconductor process technology. It produces planar components with polymer materials by duplicating a pattern formed on a mask. Among imprinting technologies, the hot embossing method is a cheap processing technology available for massive production.[4,5] Many researchers have been studying and developing it to use not only for an optical waveguide devices but also for biocomponents, micro-electromechanical systems (MEMS), and so on. Since the polarization characteristics of polymer such as absorption loss and birefringence have been improved greatly, it does not show a notable difference from the silica commonly used for waveguide materials.[4,6]

In the present study, we designed a wavelength-independent coupler (WINC), one of the planar waveguide components, with a hot embossing imprint technique and tried to optimize the size of the polymer core in the WINC. It can be located at the front end of optical communication multiplexers and used over the 1310- and 1550-nm range, and it influences wavelength characteristics of the multiplexer. Even though WINC can be fabricated using a fusion splicing method with optical fibers, that method is much more difficult than the hot embossing method.[7,8] The polymeric WINC, which has a flat transmission 50 : 50 branching fraction from 1260 to 1640 nm, was designed and then fabricated with the hot embossing method. The optical properties of the polymeric WINC were measured and compared to values from a simulation.

2 Design of WINC

Two common designing methods are used for the planar WINC: one uses the Mach–Zehnder interferometer, and the other is the taper method for the waveguide of the coupling zone. It has been discovered that when using the Mach–Zehnder interferometer, the optical characteristics of the coupler are especially well matched with the designed values. Thus, we designed the WINC with Mach–Zehnder interferometer using the beam propagation method for
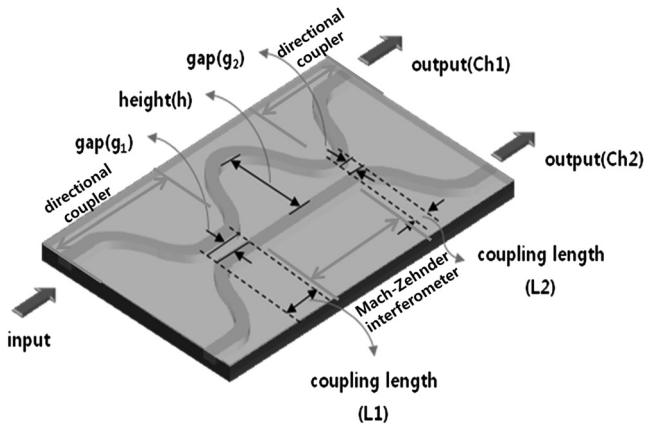
**Fig. 1** The wavelength-independent coupler based on the Mach–Zehnder interferometer.

accurate simulation of a curved structure. The structure of the WINC, shown in Fig. 1, consists of two directional couplers and two different optical paths designed in a Mach–Zehnder type. The operational principle is based on the suppression of the monotonic increase of the coupling ratio along the wavelength by creating a phase difference between the two directional couplers. In addition, we designed the 3dB coupler by computing the transfer matrix of a couple of straight waveguides based on the coupled mode theory. The transfer matrix can be expressed as Eq. (1), representing the multiplication of the 3dB coupler and transfer matrix of the optical channel difference:[9]

$$T_{WINC} = T_{3dB1} \cdot T_{\Delta L} \cdot T_{3dB2}. \tag{1}$$

T_{WINC} is the total transfer matrix of the WINC, where T_{3dB1} and T_{3dB2} are the transfer matrix of the 3dB couplers for the front and the back ends, respectively, and $T_{\Delta L}$ is the transfer matrix of the Mach–Zehnder interference. Equation (1) for T_{WINC} can be expressed in detail as in Eq. (2), with the transfer matrix of an ideal 3dB coupler and the transmission constant, where β is the propagation constant and ΔL is the optical path difference:
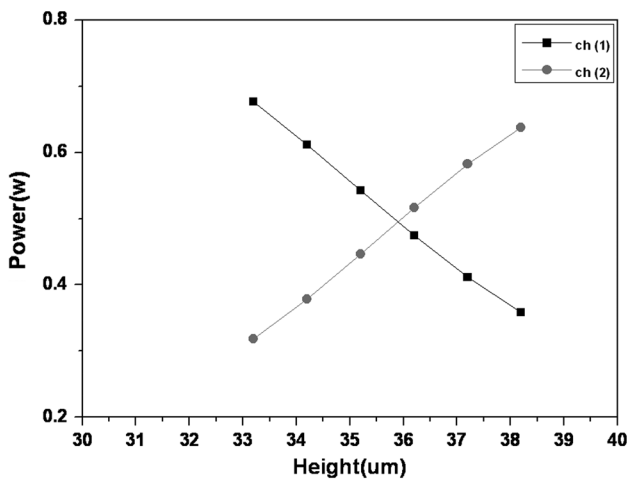
$$T_{WINC} = \frac{1}{\sqrt{2}} \begin{bmatrix} 1 & -j \\ -j & 1 \end{bmatrix} \cdot \begin{bmatrix} \exp(-j\beta \cdot \Delta L) & 0 \\ 0 & 1 \end{bmatrix}$$
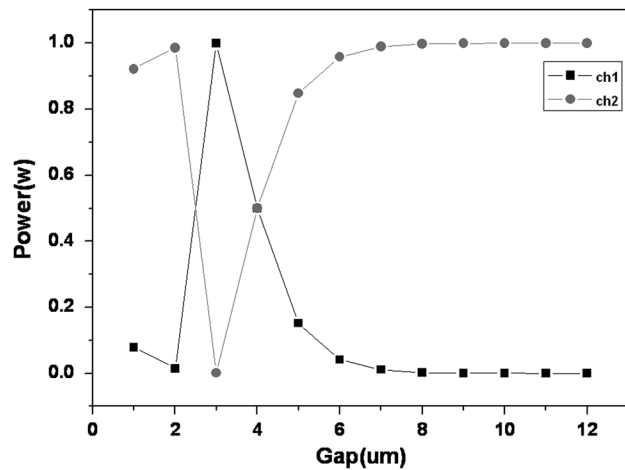$$\cdot \frac{1}{\sqrt{2}} \begin{bmatrix} 1 & -j \\ -j & 1 \end{bmatrix}. \tag{2}$$
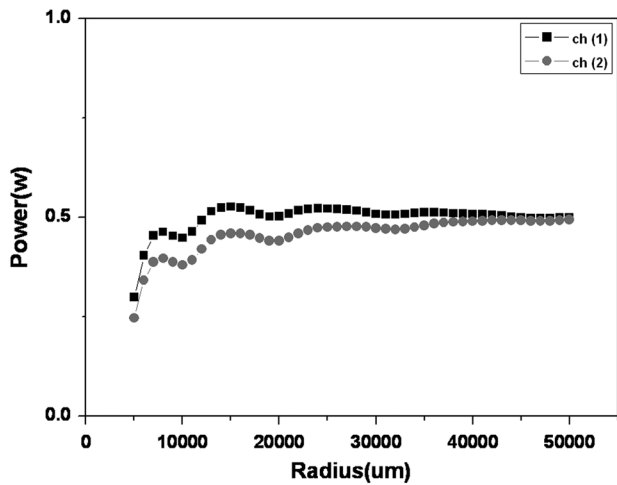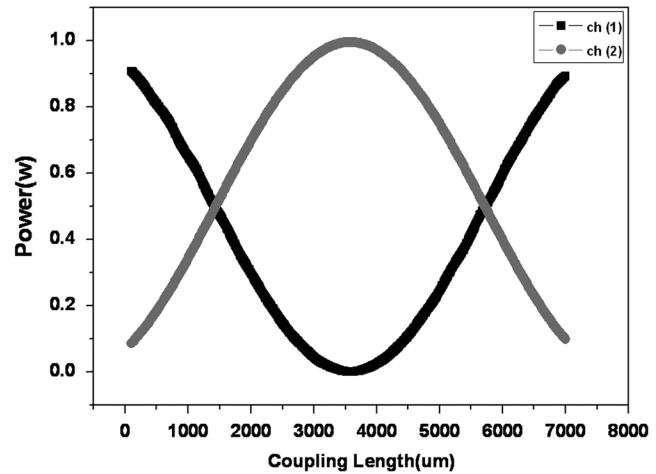
Fig. 2 Simulation results according to radius of curvature (a), coupling length (b), arm height (c), and gap of two waveguides (d).

If the optical power is incident to a port, the output intensity will be calculated with Eq. (3):

$$\begin{bmatrix} R \\ s \end{bmatrix} = T_{\text{WINC}} \cdot \begin{bmatrix} 1 \\ 0 \end{bmatrix} = \frac{1}{2} \begin{bmatrix} -1 + e^{-j\phi} \\ -j - je^{-j\phi} \end{bmatrix}. \qquad (3)$$

If Eq. (3) is expressed as an optical power equation, it will be $RR^* = \sin^2(0.5\phi)$ or $SS^* = \cos^2(0.5\phi)$, where ϕ is the phase difference caused by the optical path difference. The optical path difference ΔL can be expressed by Eq. (4):

$$\Delta L = \frac{\lambda^2}{2n_{\text{eff}}\Delta\lambda}, \qquad (4)$$

where λ is optical wavelength and n_{eff} is the effective refractive index of the polymer waveguide.

The important factors with regard to this structure are the coupling ratio of the two directional couplers and the phase difference created by the optical path difference. Thus, the coupling ratio of the directional coupler was determined by the coupling length and the distance between two separated waveguides. The optical path difference was determined by the height of the Mach–Zehnder interferometer, as shown in Fig. 1. In addition, the core size of the waveguide WINC was 8×8 μm, because the core of the waveguide needed to have a mode diameter identical to that of the optical fiber in the single mode used for the connection. Polymethyl methacrylate (PMMA) was used as a cladding material, and the refractive index was 1.4816. The resin (WIR30-490) of ChemOptics was used as the core material; its refractive index was 1.4862 (at 1310 nm). A 0.3% difference existed between the refractive indexes of the two substances. S-bends were mainly used for the curves.

Figure 2 shows the simulation results with varying the curvature radius, coupling length (L1, L2), arm height (h), and waveguide gap (g1, g2) in terms of the coupling losses. As shown in Fig. 2(a), the power of channels 1 and 2 were almost the same when the curvature radius was more than 40,000 μm. We set the radius of curvature at 50,000 μm because we considered the tolerances of curvature manufacturing process. We also set 4 μm for the waveguide gap (g1, g2), 1420 μm for the coupling length L1, 200 μm for L2, and 36 μm for the arm height (h). The optical powers of channels 1 and 2 simulated in regard to the wavelengths from 1260 to 1640 nm are presented in Fig. 3. After normalizing, the power in results was suitable for a 3dB broadband coupler, because the power values for channels 1 and 2 were almost same at $1260 \sim 1640$ nm wavelength.

When the polymer waveguide is fabricated with the hot embossing method, the core size is usually changed. Thus, we performed a power simulation for that changed core size of the waveguide from 7.9 to 8.1 μm. As shown in Fig. 4, the allowable structure size tolerance was up to ± 0.3 μm, which might be acceptable for insertion losses occurring in the WINC.

3 Fabrication and Experimental Results

We fabricated a WINC with the hot embossing method with polymer. For the hot embossing process, which is one of the most flexible and appropriate methods for fabrication of polymer optical devices,[5] a molding master is necessary. To make a master, generally processes such as the
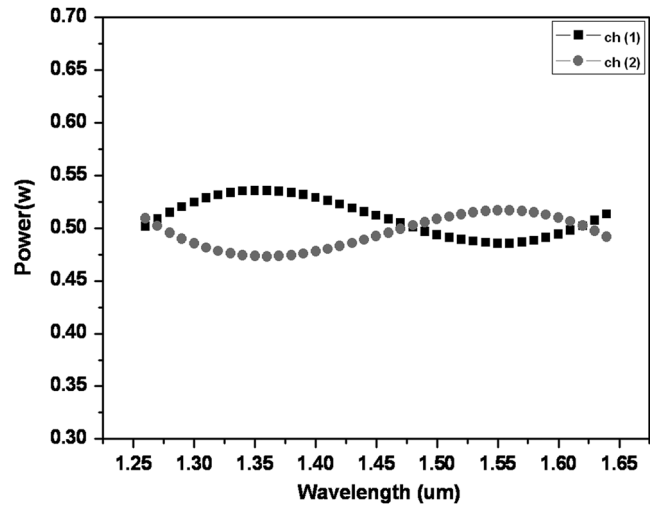

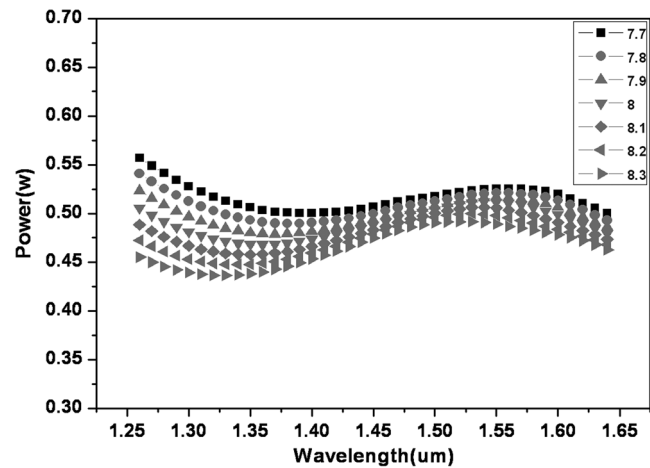Fig. 3 Optical power according to wavelength.

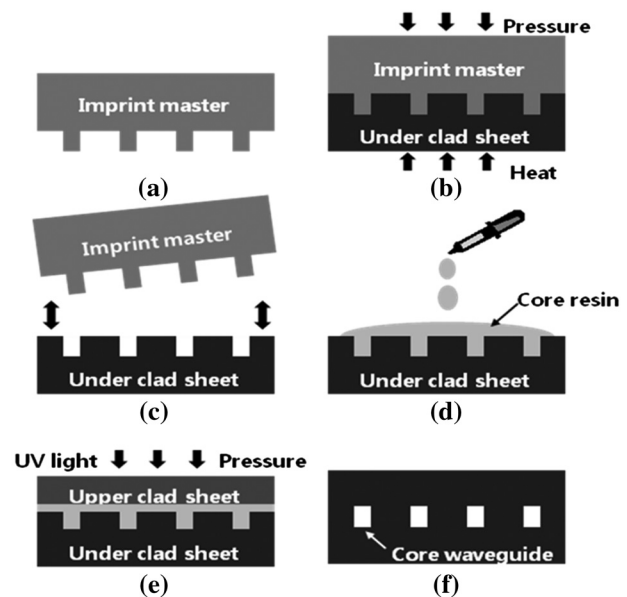Fig. 4 Simulation results according to waveguide size.

Fig. 5 Fabrication process of the polymeric WINC device: silicon master (a), hot embossing process (b), demolding master (c), core filling (d), UV curing (e), and final structure (f).

lithography, electroplating, and molding (lithographie galvanoformung abformung) process, the Bosch process, and the deep reactive ion etching (DRIE) method are applied.[10–12] In this study, we used the DRIE to make a silicon molding master. Figure 5 illustrates in detail the hot embossing process flow for the fabrication of the WINC. The hot embossing method consisted of several processing steps of imprinting by pressing a silicon master into the PMMA sheet. First, a cleaned silicon master was prepared as shown in Fig. 5(a). Second, the master was impressed onto the PMMA sheet using a hot embossing method with three steps as shown in Fig. 5(b). The three steps of the hot embossing are as follows. The temperature, pressure, and time were 140°C, 16 bar, and 60 s for the first step; 140°C, 25 bar, and 80 s for the second step; and 140°C, 16 bar, and 60 s for the third step. After these steps, the master was removed as shown in Fig. 5(c).

At that time, the temperature was set to 70°C. Figure 5(d) shows the core resin filled over the formed pattern. Figure 5(e) describes the solidification process; the core resin was solidified with 15-bar nitrogen pressure and exposed for 10 min to UV light after being covered with an upper clad sheet. Figure 5(f) shows the fabricated WINC device. To evaluate the size of optical waveguides of the fabricated WINC, we took a scanning electron microscope (SEM) image of the surface of the WINC. The size of the optical waveguide of the WINC was 8×8 μm, as shown in Fig. 6.

The optical characteristics of the fabricated WINC, such as propagation loss, insertion loss, and power uniformity in a broadband range, were evaluated. Figure 7 illustrates the schematics of the measurement. A tunable light source producing 1310- to 1550-nm wavelengths was used; the single-mode fiber was aligned with the input port of the polymeric WINC to evaluate the characteristics of the fabricated device. A multimode fiber was connected to the output port of the device; the output power was measured by a power meter (Newport, 1835-C). The broadband characteristics of the WINC were observed by an optical spectrum analyzer
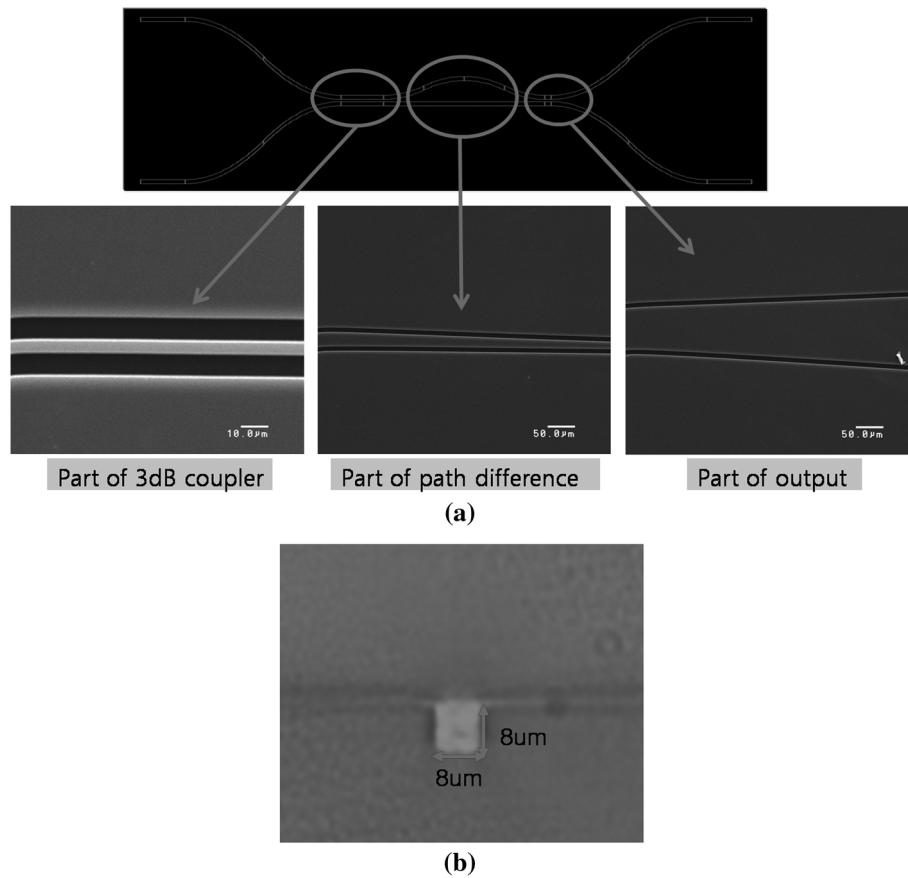

Part of 3dB coupler · Part of path difference · Part of output

(a)

8um
8um

(b)

Fig. 6 (a), SEM images for several parts of the WINC device. (b), Cross-sectional view of the optical waveguide.

(Light source) · (WINC) · (Fiber(MMF)) · (Power Meter & OSA)
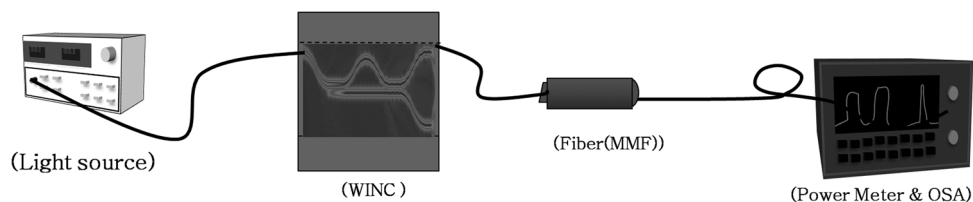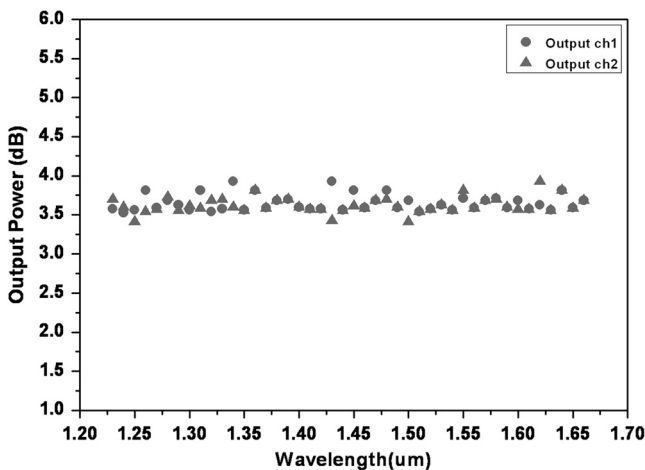
Fig. 7 Schematics of test setup.

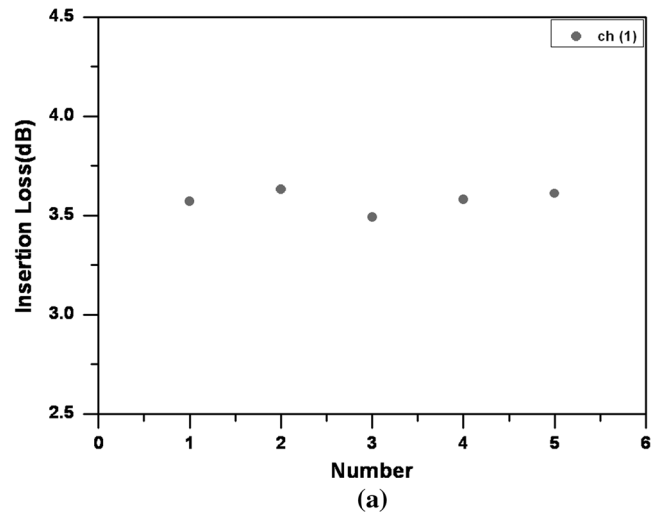**Table 1** Optical power (dB) at the output ports.

Input wavelength	Optical power at channel 1	Optical power at channel 2
1310 nm	3.6	4.2
1550 nm	3.4	4.1

(OSA, ANDO, AQ6417B). The displayed characteristics of each broadband wavelength ranged from 1260 to 1640 nm. To evaluate the propagation loss of the WINC, we constructed the straight waveguide with the same polymer using the hot embossing method. The optical power of the light source from the input fiber was 6.76 dBm (at 1310 nm), and the power of the light from the out fiber was 6.31 dBm after running the 2-cm straight waveguide and 6.53 dBm after running the 1-cm straight waveguide. Therefore, the propagation loss of the WINC was about 0.23 dB/cm.

The insertion loss can be defined as $-10\log(P_2/P_1)$ and $-10\log(P_3/P_1)$, where P_1 is the optical power of the incident light of the WINC and P_2 and P_3 are the optical power at the output ports after the light passes through the coupler. The output power at the output ports is presented in Table 1. To ensure the accuracy of the measurement of the insertion loss, two kinds of light sources (1310 and 1550 nm) were used. The results were average values of five measurements. The evaluated bandwidth of the WINC is shown in Fig. 8. The result was the 50:50 split ratio at $1260 \sim 1640$ nm. Therefore, the basic characteristics of the WINC were confirmed. The insertion losses of channel 2 were slightly bigger than those of channel 1 and also different from the simulation results. However, such differences could be ignored because of process tolerance and measurement errors. All optical characteristics of the fabricated WINC did satisfy the requirements of Telcoria–GR1209 core. We measured the devices for 5 h and confirmed the excellent stability of the device, as shown in Fig. 9. Therefore, we think that it is suitable for the optical communication system.

Fig. 9 Insertion loss changes after 5 h at port 1 (a) and port 2 (b).

4 Conclusions

We designed a WINC, usable for broadband wavelengths from 1260 to 1640 nm, using a beam propagation method based on the coupled mode theory. The coupling length, waveguide gap, and waveguide interval conditions were optimized through simulations. We fabricated the designed device using the hot embossing method that employs a nanoimprint lithography, and we evaluated its optical characteristics through the experiment. The measured propagation loss of the fabricated device was about 0.2 dB/cm. The insertion loss was measured to be 3.6 dB on channel 1 and 4.2 dB on channel 2. The output characteristics of the fabricated device were almost identical in the range from 1260 to 1640 nm, which proves its usefulness for FTTH. We expect that the proposed design and fabrication method will be applied for the development of optical switches, optical modulators, WDM optical components, and electro-optic circuit boards and make those better than other methods.

Fig. 8 Splitting characteristics according to wavelength.

References

1. Y. Xu, "Polymer planar waveguide device using inverted channel structure with upper liquid crystal cladding," *Opt. Express* **17**(10), 7837–7843 (2009).
2. K.-J. Kim et al., "Flexible polymer waveguide tunable lasers," *Opt. Express* **18**(8), 8392–8399 (2010).
3. J. Halldorsson et al., "High index contrast polymer waveguide platform for integrated biophotonics," *Opt. Express* **18**(15), 16217–16226 (2010).
4. D.-H. Kim et al., "Polymeric microring resonator using nanoimprint technique based in a stamp incorporating a smoothing buffer Layer," *IEEE Photon. Technol. Lett.* **17**(11), 2352–2354 (2005).
5. T. Balla, S. M. Spearing, and A. Monk, "An assessment of the process capabilities of nanoimprint lithography," *J. Phys. D Appl. Phys.* **41**(17), 17401–17411 (2008).
6. M.-C. Oh et al., "Integrated photonic devices incorporating low-loss fluorinated polymer materials," *Polymers* **3**(3), 975–997 (2011).
7. J. Van Campenhout et al., "Low-power, 2×2 silicon electro-optic switch with 110-nm bandwidth for broadband reconfigurable optical networks," *Opt. Express* **17**(26), 24020–24029 (2009).
8. N.-S. Son et al., "Near-infrared tunable lasers with polymer waveguide Bragg gratings," *Opt. Express* **20**(2), 827–834 (2012).
9. S. Garcia-Blanco and J. S. Aitchison, "Direct electron beam writing of optical devices on Ge-doped flame hydrolysis deposited silica," *IEEE J. Sel. Top. Quantum Electron.* **11**(2), 528–538 (2005).
10. D. Weiland et al., "Optical fibre array manufacture using electrostatic actuation," in *IEEE Advanced Packaging Materials: Microtech*, 2010 International symposium, pp. 92–97 (2010).
11. S. W. Youn et al., "Prototype development of a roller imprint system and its application to large area polymer replication for a microstructured optical device," *J. Mater. Proc. Technol.* **202**(1–3), 76–85 (2008).
12. S. W. Ahn et al., "Polymeric wavelength filter based on a Bragg grating using nanoimprint technique," *IEEE Photon. Technol. Lett.* **17**(10), 2122–2124 (2005).

Kyung Su Jang received his BS degree from Pusan University of Foreign Studies and MS degrees from Pusan University, Busan, Korea, in 2007 and 2010, respectively. He is currently working toward the PhD degree in Pusan National University, Busan, Korea. His research interests are passive optical devices and optical interconnection.

Eung Soo Kim received his BS and MS in electronics engineering from Kyungpook National University, Korea, in 1990 and 1992. He received the PhD degree in material science from Faculty of Science and Technology, Keio University, in Japan in 1996. He has been a visiting professor in Department of Electronics Engineering at Keio University in Japan as a JSPS fellowship in 2003. He has been the head of the Institute of Information & Communication in Pusan University of Foreign Studies from 2008 to 2010. He is currently a professor in Division of Digital Media Engineering, Pusan University of Foreign Studies. His research interests are optical sensors, nonlinear optics, optical waveguide devices, polymer optical fibers, and optical integrated circuits.

Chang Seok Kim received his BS degree from Korea Advanced Institute of Science and Technology, Daejeon, Korea, in 1996, the MS degree from Gwangju Institute of Science and Technology, Gwangju, in 1999, and the PhD degree from Johns Hopkins University, Baltimore, MD, in 2004. From 1999 to 2000, he was a research engineer with the Wavelength Division Multiplexing Optical Communication Team of Korea Telecom, Daejeon. His work was supported by the Korean Government Overseas Study Scholarship. In 2004 and 2005, he was a postdoctoral researcher with Beckman Laser Institute and Medical Clinic, University of California, Irvine. He joined Pusan National University, Busan, in 2005 as an assistant professor. Since 2009, he has been an associate professor in the Department of Cogno-Mechatronics Engineering, Pusan National University. His research interests include development of novel fiber laser systems and their application into biomedical, telecommunication, and sensor areas.

Myung Yung Jeong received BS and MS degrees from Pusan National University, Pusan, Korea, in 1982 and 1984, and the PhD degree from the Korea Advanced Institute of Science and Technology, Daejeon, Korea, in 2000. Since September 1983, he has worked for the Electronics and Telecommunications Research Institute, Daejeon, Korea. He is currently a professor in the Department of Cogno-Mechatronics Engineering, Pusan National University. His present research interests include imprinted optical devices, nanophotonics, optical interconnection, and optical components for in-vehicle networks.